Communication

Equivalency of Binding Sites in Protein–Ligand Complexes Revealed by Time-Resolved Tandem Mass Spectrometry

Glen K. Shoemaker, Elena N. Kitova, Monica M. Palcic, and John S. Klassen

J. Am. Chem. Soc., **2007**, 129 (28), 8674-8675• DOI: 10.1021/ja068421p • Publication Date (Web): 20 June 2007

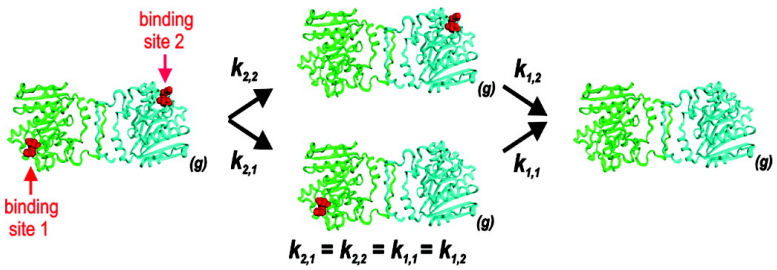

More About This Article

Additional resources and features associated with this article are available within the HTML version:

- Supporting Information
- Links to the 3 articles that cite this article, as of the time of this article download
- Access to high resolution figures
- Links to articles and content related to this article
- Copyright permission to reproduce figures and/or text from this article

View the Full Text HTML

J|A|C|S
COMMUNICATIONS

Published on Web 06/20/2007

Equivalency of Binding Sites in Protein−Ligand Complexes Revealed by Time-Resolved Tandem Mass Spectrometry

Glen K. Shoemaker,[†] Elena N. Kitova,[†] Monica M. Palcic,[‡] and John S. Klassen*,[†]

Department of Chemistry, University of Alberta, Edmonton, Alberta, Canada T6G 2G2, and Carlsberg Laboratory, Gamle Carlsberg Vej 10, 2500 Valby, Denmark

Received November 23, 2006; E-mail: john.klassen@ualberta.ca

The electrospray ionization mass spectrometry (ES-MS) assay is an established method for determining the binding stoichiometry and affinity of protein−ligand interactions, as well as other noncovalent biological complexes, in solution.[1] While the relationship between the higher order structure of protein complexes in solution and in the gas phase remains hotly debated, there is growing evidence that elements of higher order structure, including the specific intermolecular interactions, are preserved during the ES/desolvation process.[2] This raises the exciting possibility of combining ES-MS and gas-phase methods, in particular dissociation techniques, to gain insight into the nature of protein−ligand interactions present in solution. Here, we show for the first time that the number of equivalent ligand binding sites within proteins and multi-subunit protein complexes in solution can be established by time-resolved thermal dissociation experiments performed on the gaseous protein−ligand complexes.

The gas-phase assay is demonstrated for three model protein complexes. The homodimer of the human ABO(H) blood group B glycosyltransferase (GTB_2) binding with its acceptor substrate, the disaccharide α-L-Fuc*p*-(1 → 2)-*β*-D-Gal*p*-O$(CH_2)_7CH_3$ (**1**), and the homotetramer streptavidin (S_4) binding the small molecule ligand biotin (**2**) serve as positive controls, while the homodimer of wheat germ agglutinin (WGA_2) binding to *β*-D-GlcNAc*p*-(1 → 6)-D-Gal*p* (**3**) serves as a negative control. Gaseous ions of the protein−ligand complexes are produced by nanoflow ES (nanoES) performed on buffered aqueous solutions containing protein and ligand. Rate constants for the loss of ligand from the gaseous ions are determined from time-resolved thermal dissociation experiments, implemented using the blackbody infrared radiative dissociation (BIRD) technique,[3] which are carried out on a Fourier-transform ion cyclotron resonance mass spectrometer.

GTB exists exclusively as a noncovalent homodimer (GTB_2) in aqueous solution at neutral pH and 25 °C and possesses two equivalent binding sites for **1**, each with an intrinsic affinity (K_{assoc}) of 1.7×10^4 M^{-1}.[4,5] NanoES-MS performed on an aqueous solution of GTB_2 (7 μM) and **1** (40 μM) and 50 mM ammonium acetate yields ions corresponding to protonated GTB_2 bound to $q = 0-2$ molecules of **1**, that is, $(GTB_2 + q\mathbf{1})^{n+}$, at $n = 14-16$ (Figure S1, Supporting Information). Using a newly developed method for identifying nonspecific protein−ligand complexes formed during the ES process,[6] it was confirmed that the $(GTB_2 + \mathbf{1})^{n+}$ and $(GTB_2 + 2(\mathbf{1}))^{n+}$ ions arise exclusively from specific binding in solution.

BIRD of the $(GTB_2 + q\mathbf{1})^{15+}$ ions proceeds by the sequential loss of neutral **1** (Figure S2). From BIRD mass spectra acquired at different reaction times, it is possible to evaluate the reaction kinetics. Shown in Figure 1 are kinetic data, plotted as the natural log of the normalized intensity of the reactant ion (I/I_o) versus reaction time, measured for the $(GTB_2 + \mathbf{1})^{15+}$ ion. Notably, the kinetic plots are linear, which is the expected behavior for the unimolecular dissociation of a single reactant, over the range of temperatures investigated. Since both ligand binding sites are populated with equal probability in solution, the linear kinetic plots indicate that the dissociation rate constants for the loss of **1** from each of the binding sites are equivalent. Linear kinetic plots are also obtained for the loss of **1** from the $(GTB_2 + 2(\mathbf{1}))^{15+}$ ion (Figure S3), a result which is consistent with the operation of parallel dissociation pathways from a single reactant.

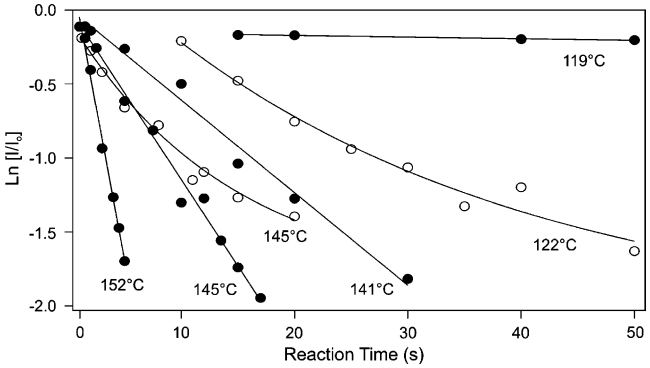

Figure 1. Plots of natural logarithm of normalized intensity (I/I_o) of the gaseous $(GTB_2 + \mathbf{1})^{15+}$ ions, produced from the specific $(GTB_2 + \mathbf{1})$ complex (●) and from a mixture of specific and nonspecific $(GTB_2 + \mathbf{1})$ complexes (○), versus reaction time, at the temperatures indicated.

At higher concentrations of **1**, >80 μM, nonspecific binding of **1** to GTB_2 is extensive and $(GTB_2 + 3(\mathbf{1}))^{n+}$ and $(GTB_2 + 4(\mathbf{1}))^{n+}$ ions are detected (Figure S1). Under these conditions, both specific and nonspecific complexes contribute to the $(GTB_2 + q(\mathbf{1}))^{n+}$ ion signals. Nonlinear kinetic plots were obtained for the $(GTB_2 + q\mathbf{1})^{15+}$ ions produced under conditions where nonspecific binding of **1** to GTB_2 occurs (Figure 1). The nonlinear kinetic plots can be explained by the presence of multiple, nonequivalent reactant ions, consistent with the contribution of both specific and nonspecific interactions to the $(GTB_2 + q\mathbf{1})^{15+}$ ions.

From the Arrhenius plots constructed for the loss of **1** from the $(GTB_2 + \mathbf{1})^{15+}$ and $(GTB_2 + 2(\mathbf{1}))^{15+}$ ions originating from specific complexes, it is evident that $(GTB_2 + \mathbf{1})^{15+}$ is kinetically more stable than $(GTB_2 + 2(\mathbf{1}))^{15+}$ (Figure S4). However, the activation energies are indistinguishable within experimental error, 58 kcal mol^{-1}. Over the temperature range investigated, the average ratio of dissociation rate constants for the loss of **1** from the $(GTB_2 + 2(\mathbf{1}))^{15+}$ and $(GTB_2 + \mathbf{1})^{15+}$ ions is 2.3 ± 0.3. This ratio agrees, within error, with the value of 2 expected on the basis of the difference in the number of equivalent bound ligands in the two ions, that is, the ligand occupancy factor.

BIRD was also applied to the complex of S_4 with biotin, **2**. In aqueous solution at pH 7, S_4 binds to four molecules of **2** with a K_{assoc} estimated to be on the order of 10^{13} M^{-1} at 25 °C.[7] Analysis

[†] University of Alberta.
[‡] Carlsberg Laboratory.

10.1021/ja068421p CCC: $37.00

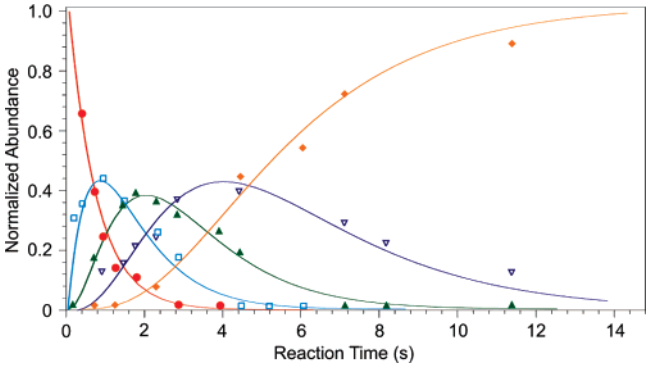

Figure 2. Breakdown curves for the sequential loss of **2** from the $(S_4 + 4(\mathbf{2}))^{13+}$ ion at a reaction temperature of 133 °C; The symbols (● = $(S_4 + 4(\mathbf{2}))^{13+}$), □ = $(S_4 + 3(\mathbf{2}))^{13+}$), ▲ = $(S_4 + 2(\mathbf{2}))^{13+}$), ▽ = $(S_4 + 1(\mathbf{2}))^{13+}$), ◆ = $(S_4)^{13+}$) represent experimental BIRD data and the solid curves represent the expected breakdown curves based on four equivalent binding sites with an intrinsic dissociation rate constant of 1.4 s^{-1}.

of the crystal structure of the $(S_4 + 4(\mathbf{2}))$ complex reveals four identical ligand binding sites.[8] NanoES-MS performed on an aqueous solution of S_4 (5 μM) and **2** (25 μM) reveals exclusively S_4 ions bound to four molecules of **2**, that is, $(S_4 + 4(\mathbf{2}))^{n+}$, at n = 14−16 (Figure S5). At temperatures ≤ 138 °C, BIRD of the $(S_4 + q(\mathbf{2}))^{n+}$ ions proceeds by the loss of both neutral and protonated **2** (Figure S6). Because of the influence of Coulombic repulsion on the dissociation kinetics, the equivalency of the ligand binding sites cannot be established from a comparison of the rate constants for the loss of neutral and protonated **2** (Figure S7). However, the charged ligand pathway can be eliminated by reducing the charge state of the $(S_4 + q\mathbf{2})^{n+}$ ions through the addition of a base to the nanoES solution.[9] For example, the $(S_4 + 4(\mathbf{2}))^{13+}$ ion dissociates exclusively by the sequential loss of neutral **2**. Shown in Figure 2 are the breakdown curves for the successive loss of **2** from $(S_4 + 4(\mathbf{2}))^{13+}$ measured at 133 °C. Also shown are the theoretical curves which were calculated from the rate constant (k_1) measured for the loss of one molecule of **2** from $(S_4 + 4(\mathbf{2}))^{13+}$ and assuming that the rate constants for the successive losses of **2** differ simply by the ligand occupancy factor, that is, $k_1 = {}^4/_3k_2 = 2k_3 = 4k_4$. Agreement between the experimental and theoretical breakdown curves indicates that the intrinsic dissociation rate constants for the loss of **2** from each of the four binding sites are identical.

The equivalency of the rate constants measured for the loss of ligand from equivalent binding sites within a given complex is compelling evidence that the binding sites are structurally equivalent in the gas phase. This is the first *quantitative* experimental evidence for the preservation of elements of structural equivalency within multi-subunit protein complexes upon transfer from solution to the gas phase. However, from these data alone, it is not possible to establish whether the native structure is preserved in the gas phase or whether each binding site is similarly changed. The present findings are, perhaps, surprising given the overwhelming evidence that heating of multi-subunit protein complexes in the gas phase results in asymmetric unfolding of the subunits.[10] Such asymmetric unfolding, should it occur, would be expected to break the structural homology of the ligand binding sites and result in nonequivalent dissociation rate constants. It is probable that, at the temperatures investigated, the kinetics for ligand loss are significantly faster than the kinetics for subunit unfolding.

The homodimer WGA_2, which possesses two pairs of structurally nonequivalent binding sites for GlcNAc-containing ligands,[11] served as a negative control. NanoES-MS analysis of aqueous solutions of WGA_2 and **3** confirmed the presence of two pairs of ligand binding sites with K_{assoc} values of 4.8 ± 0.6 × 10^3 and 3.0 ± 0.5 × 10^3 M^{-1}, respectively (Figure S8). BIRD was performed on the protonated $(WGA_2 + \mathbf{3})^{n+}$ ions at n = 10 and 11. At temperatures <170 °C, $(WGA_2 + \mathbf{3})^{10+}$ dissociates exclusively by the loss of neutral **3**, while $(WGA_2 + \mathbf{3})^{11+}$ dissociates by the loss of protonated **3** (Figure S9). Notably, the kinetic plots obtained for the dissociation of both $(WGA_2 + \mathbf{3})^{n+}$ ions are nonlinear (Figure 3), which is indicative of multiple, kinetically distinct reactant ions. These results are consistent with the nonequivalent protein−ligand interactions in solution giving rise to kinetically nonequivalent interactions in the gas phase.

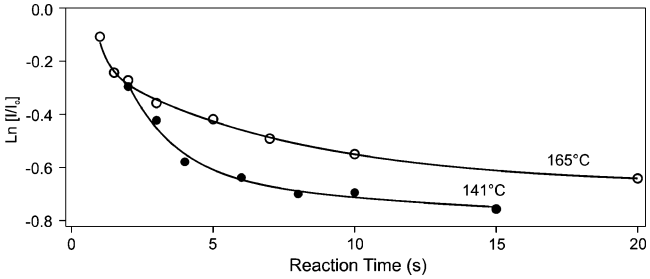

Figure 3. Plots of natural logarithm of normalized intensity (I/I_o) of the gaseous $(WGA_2 + \mathbf{3})^{11+}$ (●) and $(WGA_2 + \mathbf{3})^{10+}$ (○) ions versus reaction time, at the temperatures indicated.

In summary, we have demonstrated that, upon transfer from solution to the gas phase by ES, structurally and thermodynamically equivalent protein−ligand interactions in solution result in equivalent kinetic and energetic stabilities in the gas phase. This important finding serves as the basis for a new assay, which employs time-resolved tandem mass spectrometry, for evaluating the equivalency of ligand binding sites within proteins and multiprotein complexes in solution.

Acknowledgment. The authors are grateful for financial support provided by the Natural Sciences and Engineering Research Council of Canada and the Alberta Ingenuity Centre for Carbohydrate Science.

Supporting Information Available: Experimental section, illustrative nanoES and BIRD mass spectra, and kinetic data. This material is available free of charge via the Internet at http://pubs.acs.org.

References

(1) Daniel, J. M.; Friess, S. D.; Rajagopalan, S.; Wendt, S.; Zenobi, R. *Int. J. Mass Spectrom.* **2002**, *216*, 1−17.
(2) (a) Kitova, E. N.; Bundle, D. R.; Klassen, J. S. *J. Am. Chem. Soc.* **2002**, *124*, 9340−9341. (b) Xie, Y.; Zhang, J.; Yin, S.; Loo, J. A. *J. Am. Chem. Soc.* **2006**, *128*, 14432−14433. (c) McCammon, M. G.; Hernandez, H.; Sobott, F.; Robinson, C. V. *J. Am. Chem. Soc.* **2004**, *126*, 5950−5951.
(3) Dunbar, R. C.; McMahon, T. B. *Science* **1998**, *279*, 194−197.
(4) Shoemaker, G. K.; Palcic, M. M.; Klassen, J. S. Manuscript in preparation.
(5) Lee, H. J.; Barry, C. H.; Borisova, S. N.; Seto, N. O. L.; Zheng, R. X. B.; Blancher, A.; Evans, S. V.; Palcic, M. M. *J. Biol. Chem.* **2005**, *280*, 525−529.
(6) Sun, J.; Kitova, E. N.; Klassen, J. S. *Anal. Chem.* **2006**, *78*, 3010−3018.
(7) Chilkoti, A.; Tan, P. H.; Stayton, P. S. *Proc. Natl. Acad. Sci. U.S.A.*, **1995**, *92*, 1754−1758.
(8) Weber, P. C.; Ohlendorf, D. H.; Wendoloski, F. R.; Salemme, F. R. *Science* **1989**, *243*, 85−88.
(9) Catalina, M. I.; van den Heuvel, R. H. H.; van Duijn, E.; Heck, A. J. R. *Chem. Eur. J.* **2005**, *11*, 960−968.
(10) Benesch, J. L.; Robinson, C. V. *Curr. Opin. Struct. Biol.* **2006**, *16*, 245−251.
(11) Wright, C. S. *J. Mol. Biol.* **1984**, *178*, 91−104.

JA068421P